JOURNAL OF CATALYSIS **158,** 1–12 (1996)
ARTICLE NO. 0001

Propane Dehydrogenation over Supported Pt and Pt–Sn Catalysts: Catalyst Preparation, Characterization, and Activity Measurements

Odd A. Bariås[1], Anders Holmen, and Edd A. Blekkan

Department of Industrial Chemistry, The Norwegian Institute of Technology (NTH), N-7034 Trondheim, Norway, and SINTEF Applied Chemistry, N-7034 Trondheim, Norway

Received October 3, 1994; revised June 7, 1995

Pt and Pt–Sn catalysts supported on SiO_2 and γ-Al_2O_3 and prepared by impregnation have been studied by temperature-programmed reduction (TPR), hydrogen chemisorption, temperature-programmed desorption (TPD), and catalytic dehydrogenation of propane. Without the promoter Pt shows the same initial specific activity on both supports, but deactivates rapidly due to coking. The effect of Sn as a promoter depends on the support. On γ-Al_2O_3 tin interacts with the support and is stabilized in an oxidation state >0. The result is an increase in Pt dispersion and an improved stability of the catalytic activity without any change in the initial specific activity in dehydrogenation. On SiO_2 the Sn is more readily reduced, and alloy formation is possible. This leads to a similar increase in Pt dispersion and improved catalytic stability, but also to a strong reduction in the specific activity. The change in catalytic stability on both supports is paralleled by a dramatic change in the hydrogen adsorption properties, as seen from the TPD profiles after reduction.

INTRODUCTION

The bimetallic system Pt–Sn has been much studied as a catalyst for reforming or dehydrogenation reactions. The promotion by Sn is known to increase the lifetime of these catalysts due to reduced deactivation by coking. Several suggestions have been made to explain the effect of tin as a promoter. Increased dispersion due to tin acting as a spacer (1) or formation of ensembles of a favorable size (2) are examples of explanations based on geometric effects. It has also been suggested that tin leads to increased mobility of adsorbed hydrogen (3) or poisons acidic sites on the alumina support (1, 4). Much recent work has been focused on the state of tin in these catalysts, particularly on the oxidation state of tin and the possibility of alloy formation after reduction. A general picture is that alloying is important on SiO_2 and other supports with less interaction, see e.g., Refs. (5–7), whereas on Al_2O_3 tin is stabilized in the +2 oxidation state (5, 7, 8). However, some studies indicate the possibility of alloy formation also on Al_2O_3 supports (9–12), particularly with high Sn loadings. Bimetallic PtSn particles with tin as Sn^0 have been reported on Al_2O_3 after specialized preparation routines (13). It has been suggested that repeated coking–regeneration cycles lead to increased alloying and consequently to a reduced activity in dehydrogenation (14).

This paper presents some experimental results from a study of Pt and Pt–Sn catalysts supported on γ-Al_2O_3 or SiO_2 used in the dehydrogenation of propane to propene. We have studied catalysts prepared by a standard impregnation technique. By combining the characterization results with specific activities (turnover frequencies) in propane dehydrogenation, we aim to show the influence of tin and how possible alloying influences the activity in dehydrogenation reactions.

EXPERIMENTAL

The experimental work includes a number of different pretreatments followed by different characterization techniques and activity measurements and a summary is outlined in Fig. 1.

Catalyst Preparation

Catalysts were prepared by incipient wetness impregnation of the supports (SiO_2, Merck Kieselgel 60; γ-Al_2O_3; Kaiser Chemicals Versal 250) using distilled water as the solvent. The salts used were $H_2PtCl_6 \cdot 6H_2O$ (Alfa/Johnson Matthey) and $SnCl_2 \cdot 2H_2O$ (Merck, min. 98% purity). The Sn salt was dissolved in 6% HNO_3 solution. The bimetallic catalysts were prepared by sequential impregnation; Sn was impregnated first, the catalyst was then dried and calcined (see below), Pt was subsequently impregnated, and the drying and calcination were repeated (Fig. 1). The catalysts were dried in air at 100°C, 10–15 h. After drying, the catalysts were calcined in a fluidized bed reactor. The

[1] Present address: Falconbridge Nikkelverk, AS, P.O. Box 457, N-4601 Kristiansaud, Norway.

0021-9517/96 $12.00

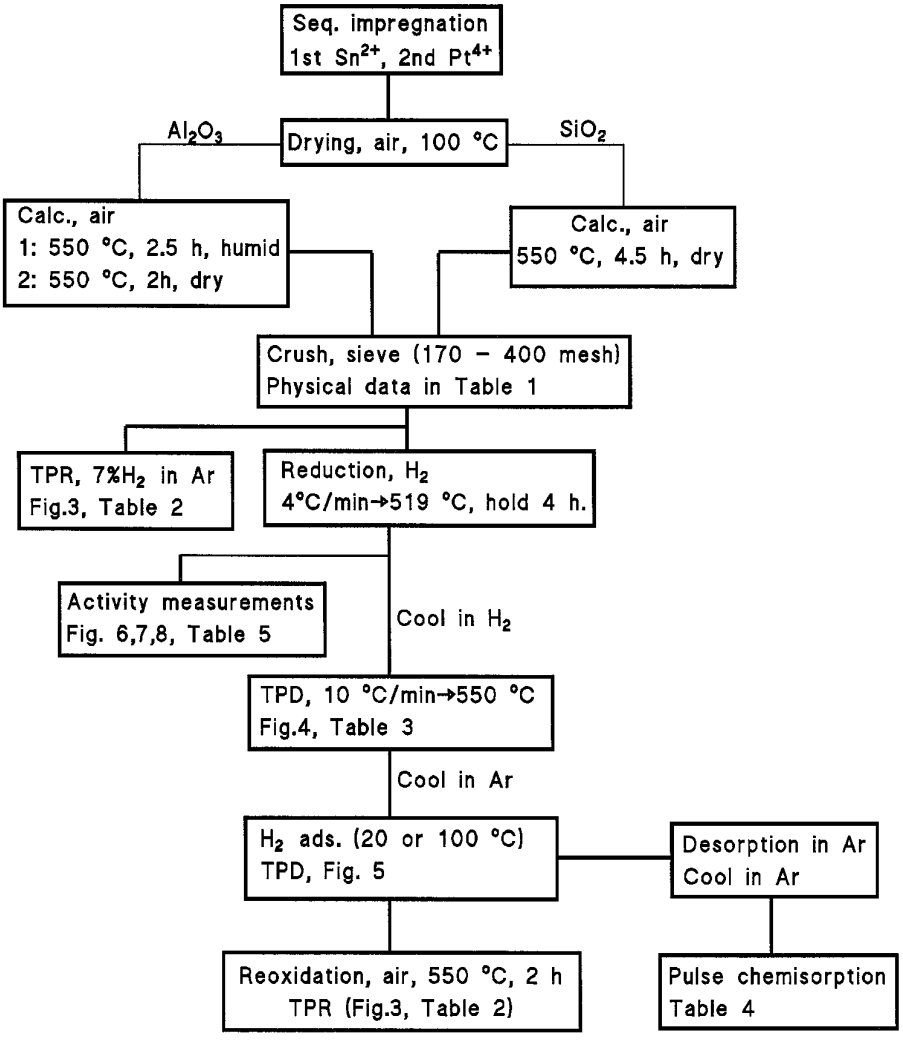

FIG. 1. Schematic representation of the catalyst preparation, characterization, and activity measurement procedures.

γ-Al_2O_3-supported samples were heated (3 K/min) to 550°C in air and calcined for 2.5 h at this temperature in humid air (P_{H_2O} = 25 kPa) and finally the wet air was replaced with dry air and the catalysts were calcined for an additional 2 h at 550°C. The SiO_2-based samples were only exposed to dry air (4.5 h at 550°C, heating rate 3 K/min). The purpose of the wet calcination was to reduce the chlorine content of the catalysts. After calcination the catalysts were crushed and sieved to 170–400 mesh. The catalyst compositions are given in Table 1. Prior to activity measurements or chemisorption/TPD experiments, the catalysts were reduced *in situ* in flowing H_2, using a heating rate of 4 K/min, up to 519°C, holding time 4 h.

Apparatus

Kinetic measurements and catalyst characterization [flow adsorption, temperature-programmed desorption (TPD), pulse chemisorption, temperature-programmed oxidation (TPO) of coked catalysts] were performed in a multipurpose apparatus shown in Fig. 2. The apparatus is designed for transient and switching experiments, and downstream of the feed-switching valves care is taken to minimize the dead volume, using narrow tubing, ''zero-dead-volume'' Valco valves and avoiding unnecessary blind-end tube connections that can disturb the flow pattern. The apparatus consists of a feed section with air-actuated selection valves (Valco) for switching between feed streams. The feed flow is controlled and metered using electronic Hi-Tec mass flow controllers. The gases are purified using combinations of oxytrap and molsieve drying columns. The reactor is a fixed-bed quartz U-tube reactor with a low dead volume (Fig. 2). The reactor effluent can be analyzed continuously by a quadrupole mass spectrometer (Balzers QMG 420) and can also be analyzed by GC for hydrocarbon content and distribution (HP5880 GC,

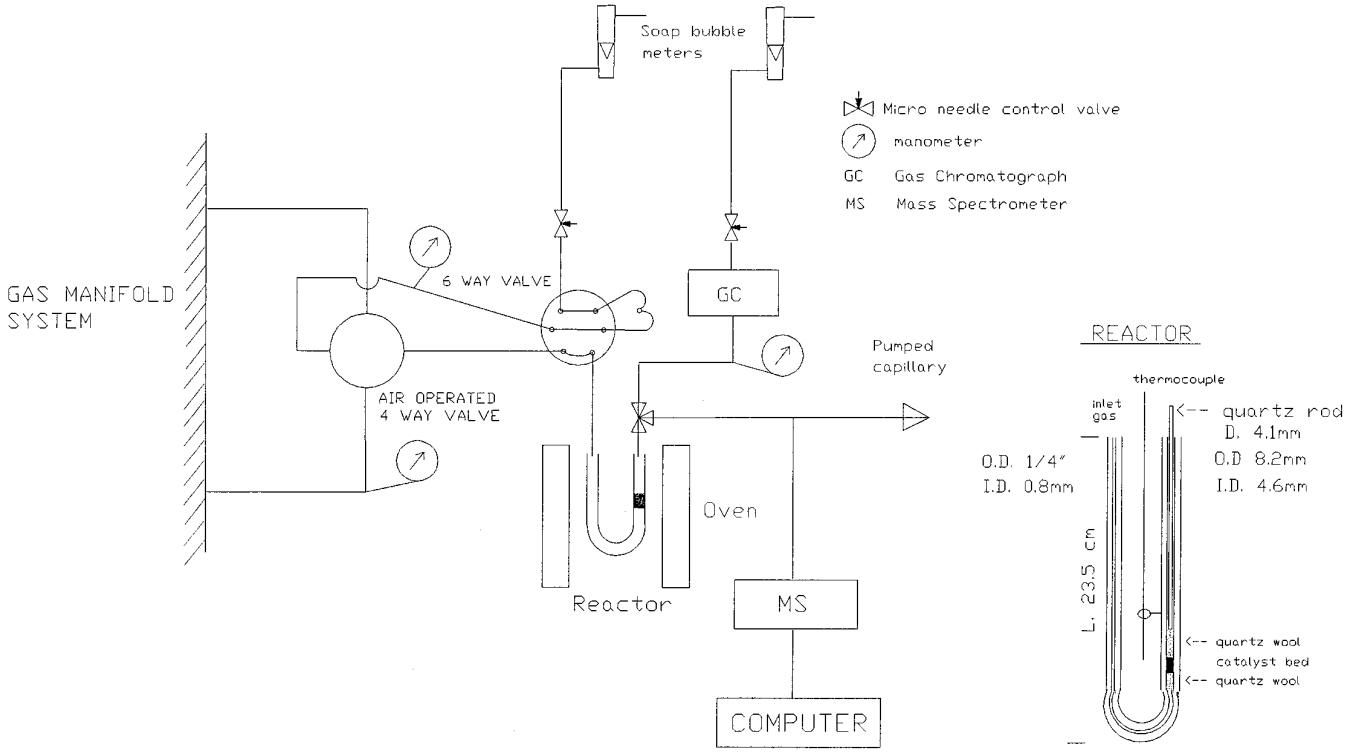

FIG. 2. Schematic drawing of the multipurpose apparatus for characterization, activity measurements, and transient kinetic studies.

equipped with a GS-alumina Megabore capillary column and a flame-ionization detector). The apparatus is equipped with a pulse valve for injection of adsorbates.

Temperature programmed reduction (TPR) experiments were performed in a standard apparatus described elsewhere (15).

Experimental Procedures

For a schematic summary of the procedures, see Fig. 1. TPR was performed on the calcined and screened samples using a 7% H_2 in Ar gas mixture, flow rate 30 ml/min, and a catalyst mass of 0.94 g. Before the run the baseline was stabilized in the gas flow at 20°C for 60 min. The heating rate was 10 K/min up to 940°C. The apparatus was calibrated by the reduction of samples of Ag_2O.

Before chemisorption and TPD experiments the catalysts were reduced as described above. The catalyst mass used in the characterization experiments was in the range 1.7–2.5 g. After the reduction the catalyst was cooled in flowing H_2. The gas stream was switched to Ar and subsequently a TPD experiment was performed (10 K/min, up to 550°C, holding time 30 min followed by cooling to 20°C in the Ar gas stream). Subsequent TPD experiments were performed after chemisorption of H_2 at 20°C or at 100°C using a fixed H_2 partial pressure (1.69 kPa). After the sample was saturated with H_2 (after 3 min) the gas was switched to pure Ar and the baseline was stabilized for 10 min before running the TPD experiment. Finally the sample was cooled and reoxidized (550°C, air, 2 h, termed ''reoxidized sample'' in the Results section) and a TPR experiment was performed as described above.

Before pulse chemisorption experiments the sample was purged in Ar at 519°C for 120 min and cooled to 20°C in flowing Ar. The pulse size was 50×10^{-3} Nml pure H_2 and the time between pulses was 4 min.

Activity measurements were performed on the reduced

TABLE 1

Composition and Surface Areas of Catalysts

Catalyst	Composition (wt%) Pt[a]	Sn[a]	Cl	S_{BET} m^2/g
γ-Al_2O_3	—	—	n.m.[b]	308
SiO_2	—	—	n.m.	483
Pt/γ-Al_2O_3	0.44	—	0.48	180
PtSn/γ-Al_2O_3	0.35	1.26	0.68	155
Sn/γ-Al_2O_3	—	1.26	n.m.	164
Pt/SiO_2	0.60	—	0.24	442
PtSn/SiO_2	0.60	1.20	0.36	417

[a] Nominal composition.
[b] n.m., not measured.

catalysts over 33-mg catalyst samples, using the 170–400 mesh sieve fraction (37–88 μm). The space velocity (WHSV based on propane) was between 3 and 10 h^{-1}, using a partial pressure of propane of 30.4 kPa, with N_2 as the balance to atmospheric pressure ($C_3H_8:N_2 = 3:7$). In some experiments part of the N_2 was replaced by H_2($C_3H_8:N_2:H_2 = 3:6:1$). The reaction temperatures used were 427 or 519°C.

The absence of any influence of both external and internal mass transfer resistance on the reaction rates was checked using the standard methods (larger catalyst particles and higher linear gas flow rates with constant space velocity). In most experiments the catalyst was cooled to the reaction temperature (if necessary) in H_2 before switching directly to the reactant mixture, but in some cases (specified in the Results section) the sample was purged in an Ar stream to remove adsorbed H_2 before switching to the reactant mixture. This procedure involved switching to a pure Ar stream at the end of the reduction period and holding the catalyst at the reduction temperature (519°C) in flowing Ar for 60 min before switching to the reaction conditions.

The gases used in the activity measurements and characterization experiments were: H_2 (purity 99.995%, Hydrogas), Ar (99.997%, Hydrogas), He (99.998%, Hydrogas), C_3H_8 (99.95, Air products), and N_2 (99.99%, Hydrogas).

TABLE 2

Degrees of Reduction Calculated from Hydrogen Consumption in the TPR Experiments

Catalyst	Degree of Pt reduction[a]		Degree of Sn reduction[b]	
	600°C	940°C	600°C	940°C
$Sn/\gamma\text{-}Al_2O_3$	—	—	25	60
$Pt/\gamma\text{-}Al_2O_3$	45	>100	—	—
$Pt/\gamma\text{-}Al_2O_3$, reoxidized	100	>100	—	—
$Pt–Sn/\gamma\text{-}Al_2O_3$	>100[c]	>100[c]	35	60
$Pt–Sn/\gamma\text{-}Al_2O_3$, reoxidized	>100[c]	>100[c]	35	65
Pt/SiO_2	70	75	—	—
Pt/SiO_2, reoxidized	70	75	—	—
$Pt–Sn/SiO_2$	>100[c]	>100[c]	80	80
$Pt–Sn/SiO_2$, reoxidized	>100[c]	>100[c]	60	60

[a] Calculated from the hydrogen consumption from the start of the experiment up to the given temperature assuming $PtO_2 + 2H_2 \rightarrow Pt + 2H_2O$, correcting for the consumption over the support alone.

[b] Calculated from the hydrogen consumption from the start of the experiment to the given temperature assuming the reaction $SnO_2 + 2H_2 \rightarrow Sn + 2H_2O$, correcting for the reduction of Pt and the support alone.

[c] The data correspond to a degree of reduction larger than 100% of Pt; 100% reduction assumed when calculating the degree of Sn reduction.

RESULTS

Temperature-Programmed Reduction

γ-Al_2O_3-based samples. Figure 3a shows TPR profiles up to 940°C of the γ-Al_2O_3-based catalysts. The integrated H_2 consumption data are shown in Table 2 in the form of calculated degrees of reduction. The catalysts all show a reduction peak at about 740°C. All the Pt-containing samples have a shoulder at lower temperatures on this peak, possibly due to a catalyzed reduction occurring at slightly lower temperatures when Pt is present, but the main high-temperature feature is centered around 740°C for all the samples. The origin of the 740°C peak is unknown, but it can be speculated that it is linked with the reduction of contaminant ions in the material. Reoxidation did not influence this feature. The $Pt/\gamma\text{-}Al_2O_3$ sample shows TPR peaks at 260 and 465°C. A negative peak can be observed at about 550°C. This is probably due to desorption of hydrogen and consequently is a similar part of the hydrogen consumption curve due to adsorption of hydrogen. These processes probably occur on the other samples as well, but are masked by the more important reduction processes that consume a larger amount of hydrogen. Table 2 shows a hydrogen consumption corresponding to a moderate degree of Pt reduction up to 600°C and a high hydrogen consumption up to 940°C. After a reduction–reoxidation cycle this picture is changed, and the hydrogen consumption up to 600°C corresponds roughly to a complete reduction of all the Pt from PtO_2 to Pt(0). The lower hydrogen consumption observed for the fresh catalyst could possibly indicate that the Pt was at least partly reduced to metallic Pt during the calcination step, as has been observed by others (16, 17), whereas the reoxidation leaves the Pt in the +4 oxidation state.

Sn alone also showed some reducibility on γ-Al_2O_3, as indicated by the broad peaks at 260°C and 405°C. However, the profiles and the consumption data for the $PtSn/\gamma\text{-}Al_2O_3$ confirm that Pt assists in the reduction of Sn, as also found by others (8, 18–21). The data in Table 2 also indicate that the Sn reduction in $PtSn/\gamma\text{-}Al_2O_3$ does not (on an average basis) extend to Sn(0), which is in agreement with the conclusions of others (1, 22–24). However, the precision of these measurements and calculations does not allow us to draw a firm conclusion on this, since it is possible that part of the Sn can be more reduced than the average numbers indicate. Reoxidation of the $PtSn/\gamma\text{-}Al_2O_3$ shifts the reduction peak to a lower temperature (105°C), but does not alter the overall H_2 consumption.

SiO_2-based samples. The TPR profiles of the SiO_2-based samples are shown in Fig. 3b. The Pt/SiO_2 catalyst shows reduction peaks at 130 and 205°C, in good agreement with the results of Ebitani and Hattori (25). The hydrogen consumption data shown in Table 2 indicate a more com-

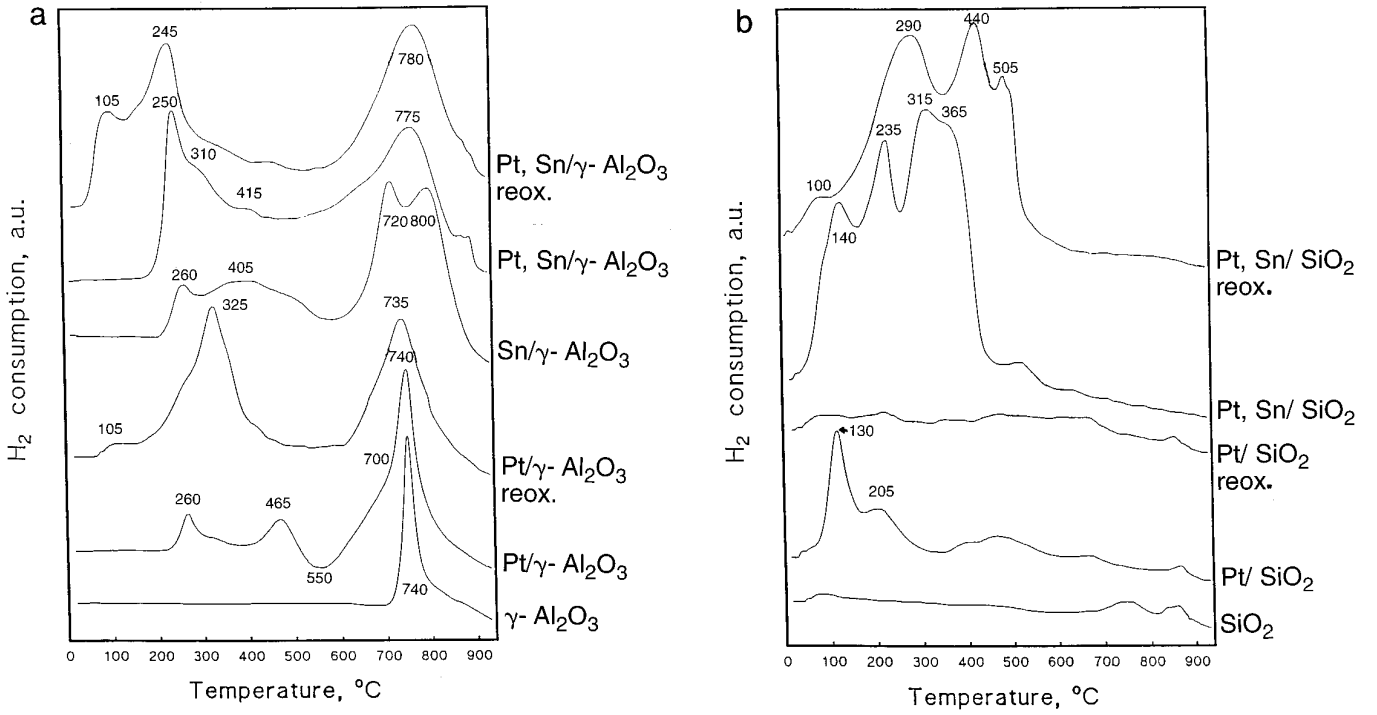

FIG. 3. TPR profiles of the catalysts: (a) γ-Al_2O_3-supported and (b) SiO_2-supported samples.

plete reduction of Pt/SiO_2 compared to Pt/γ-Al_2O_3 up to 600°C, but no further reduction processes at higher temperatures. The reoxidized sample shows no detectable hydrogen consumption. This could again be due to decomposition of the Pt oxide to metallic Pt during the oxidation step, as suggested by Lieske *et al.* (16, 26). However, a reduction during the stabilization period before the TPR run is also possible, particularly if the oxidation has led to sintering of the Pt into large, easily reduced particles (27). $PtSn/SiO_2$ shows a large H_2 consumption, and the calculations indicate a more complete reduction of Sn compared to the $PtSn/\gamma$-Al_2O_3 sample. The TPR profile is poorly resolved, and detailed assignments of reduction peaks is difficult. Reoxidation shifts and changes the peaks somewhat, without influencing the H_2 consumption significantly.

Temperature-Programmed Desorption of Hydrogen

TPD of hydrogen adsorbed during reduction and cooling in flowing H_2 is shown in Fig. 4. The amounts of desorbed hydrogen were quantified and the results are given in Table 3 as H : Pt ratios. The Sn/γ-Al_2O_3 sample showed no desorption, as also found by others (3, 28, 29). The unpromoted Pt/SiO_2 catalyst showed peaks at 80°C, at 200°C, and at the isothermal temperature (550°C). A weak feature can also be observed at 150°C. Similarly, the Pt/γ-Al_2O_3 showed peaks at 75°C, 200°C (very weak), and 550°C, but the 150°C desorption peak cannot be observed. The promoted samples were dramatically different, both showing very large, high-temperature desorption peaks at 470°C ($Pt–Sn/\gamma$-Al_2O_3, H : Pt = 4.3) and at 310°C ($Pt–Sn/SiO_2$, H : Pt = 8.6).

Figure 5 shows TPD profiles obtained after hydrogen adsorption at 20°C (Fig. 5a) and 100°C (Fig. 5b). The catalysts were saturated with H_2 (1.69 kPa) using a step-up concentration change from Ar to Ar + H_2. Before the

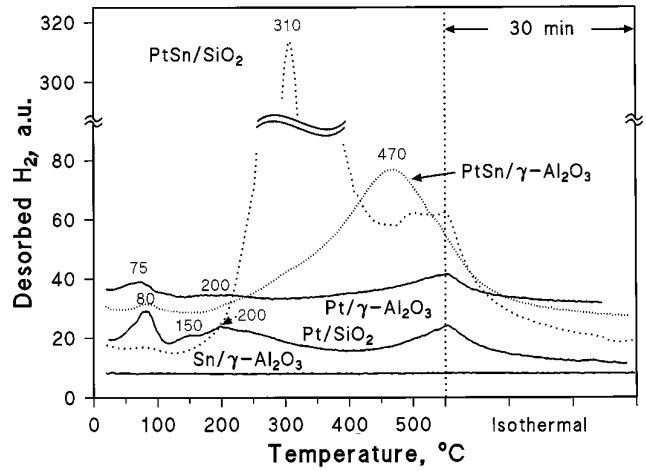

FIG. 4. TPD of hydrogen after reduction at 519°C and subsequent cooling in flowing hydrogen.

TABLE 3

Summary of Data from TPD after Reduction and Subsequent Cooling in H_2

Catalyst	TPD peak temperatures °C	Integrated amount of desorbed H per mole Pt
$Sn/\gamma\text{-}Al_2O_3$	—	—
$Pt/\gamma\text{-}Al_2O_3$	75, 200 (weak), 550[a]	0.55
$Pt–Sn/\gamma\text{-}Al_2O_3$	80, 470 (broad)	4.3
Pt/SiO_2	80, 150 (weak), 200, 550[a]	0.54
$Pt–Sn/SiO_2$	80 (weak), 310, 500–550	8.6

[a] End of temperature program.

TABLE 4

Platinum Dispersion Data from Pulse Chemisorption of H_2 at 20°C

Catalyst	Pt dispersion (H:Pt-ratio)
$Pt/\gamma\text{-}Al_2O_3$	0.17
$Pt–Sn/\gamma\text{-}Al_2O_3$	0.28
Pt/SiO_2	0.06
$Pt–Sn/SiO_2$	0.13

adsorption the samples were purged in flowing Ar at 550°C for 30 min and cooled in Ar to the adsorption temperature. After adsorption at 20°C (Fig. 5a) all the samples show desorption peaks at about 80°C, usually attributed to hydrogen on metallic Pt, and also a peak at the maximum desorption temperature, possibly indicating incomplete purging of the samples before the adsorption experiment. After adsorption at 100°C (Fig. 5b) the Pt/SiO_2 shows a larger TPD peak at 165°C, whereas the other samples show very weak features at 150–170°C.

Platinum Dispersion

Table 4 shows dispersion estimates calculated from pulse chemisorption at 20°C using the assumption H:Pt = 1 (30–32). The chemisorption results indicate that addition of Sn increases dispersion. Similar conclusions could be drawn from some of the results from other adsorption or desorption experiments discussed above, but in some cases there were differences, probably due to differences in spillover hydrogen formation. Further results from adsorption and desorption experiments are reported elsewhere (33). In general, the $\gamma\text{-}Al_2O_3$-supported samples show low dispersions compared to conventional bimetallic reforming catalysts. This is possibly due to the harsh pretreatment conditions (calcination with humid air) used in this study.

Catalytic Activity and Selectivity

Catalytic activities were measured at 427 and 519°C, both with a propane/N_2 feed and also with additional H_2 in the feed stream to reduce deactivation.

Figure 6 shows initial turnover frequencies (TOFs) for propane dehydrogenation over the catalysts at 427°C (WHSV = 10 h^{-1}, $C_3H_8:N_2$ = 3:7). With the exception of $PtSn/SiO_2$ the catalysts show initial TOFs close to 1 s^{-1}. The other major difference lies in the deactivation pattern; the unpromoted catalysts lose their activity rapidly even under these mild conditions while the Sn-promoted samples maintain their activity over an extended period of time. The $PtSn/SiO_2$ catalyst shows an initial increase in activity from a TOF of about 0.15 s^{-1} to a maximum after about 50 min on stream, where the TOF was 0.25 s^{-1}, still far lower than the initial activity of the other samples. This

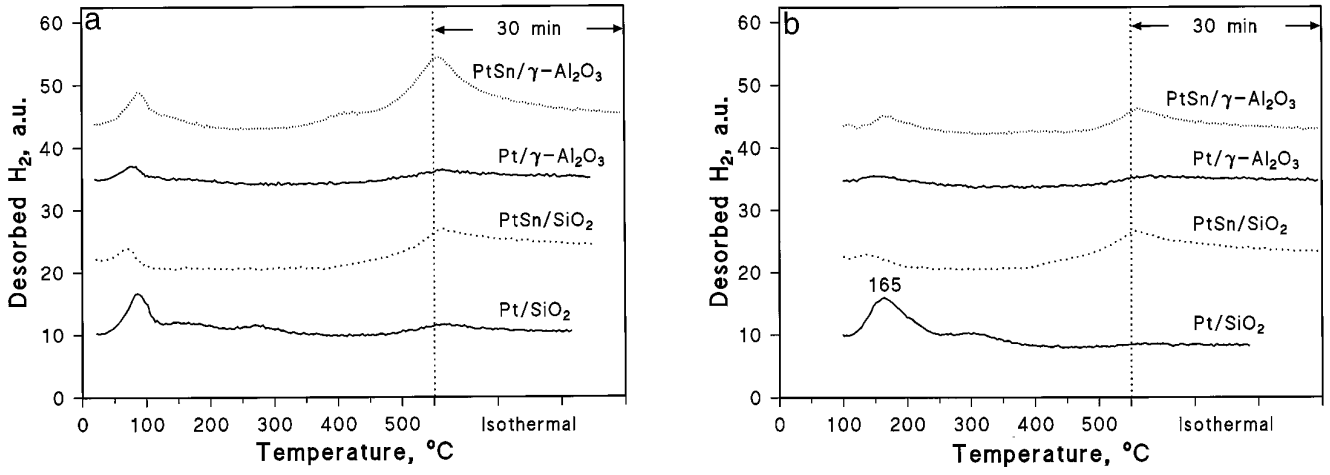

FIG. 5. TPD of hydrogen after adsorption at (a) 20°C and (b) 100°C. Before the adsorption the catalysts were purged in Ar at 550°C for 30 min and cooled to the adsorption temperaure in flowing Ar.

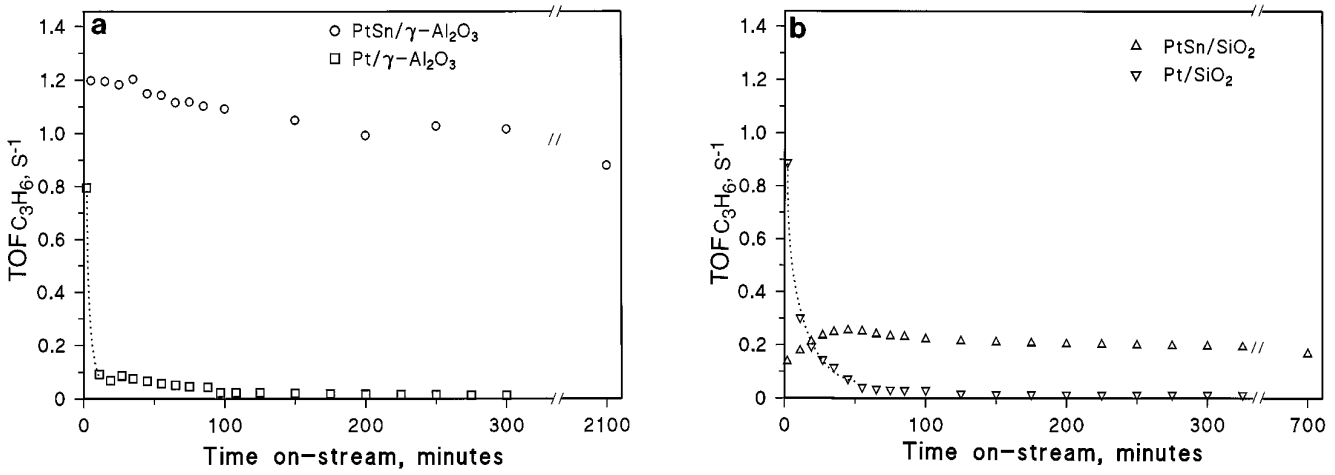

FIG. 6. Initial specific activities (TOF) of the catalysts at 427°C: (a) γ-Al_2O_3-supported catalysts, (b) SiO_2-supported samples. Conditions: WHSV = 10 h^{-1}, $C_3H_8:N_2 = 3:7$, $P_{tot} = 1$ bar.

catalyst was very stable and maintained the activity for an extended period of time. Data recorded at 519°C and under otherwise similar conditions are shown in Fig. 7. The same effects are present, but for the unpromoted catalysts the initial deactivation is so rapid that it is not possible to obtain reliable initial data.

The $PtSn/SiO_2$ shows the initial increase in the activity also at 519°C (Fig. 7b), and the maximum is reached more quickly, after about 10 min on stream. Figure 7b also includes experiments where the samples were purged with flowing Ar after reduction (solid symbols). Following reduction in H_2 at 519°C, the gas was switched to a pure Ar stream and kept at 519°C for 1 h before introducing the feed. The initial activity was now higher and declined monotonically throughout the experiment. After extended time on stream the activity level coincided with that after a normal start-up procedure. This demonstrates that the initial increase in activity with $PtSn/SiO_2$ is linked with the competitive adsorption of hydrogen, present after the catalyst reduction. The initial activity level after purging corresponds well with the maximum level reached after some time on stream, in a normal experiment, but after prolonged time on stream the activity is similar in the two cases. Over the $PtSn/\gamma$-Al_2O_3 catalyst purging with Ar using the same procedure leads to a decrease in the initial activity by about 25%, and the curves continue in parallel, the activity lost initially not being regained (Fig. 7b).

Figure 8 shows experiments at 519°C with the γ-Al_2O_3-supported samples and with H_2 in the feed (WHSV = 3.3 h^{-1}, $C_3H_8:N_2:H_2 = 3:6:1$). Figure 8a illustrates clearly that Pt and PtSn on γ-Al_2O_3 has the same initial TOF when deactivation due to coking is reduced by H_2 addition

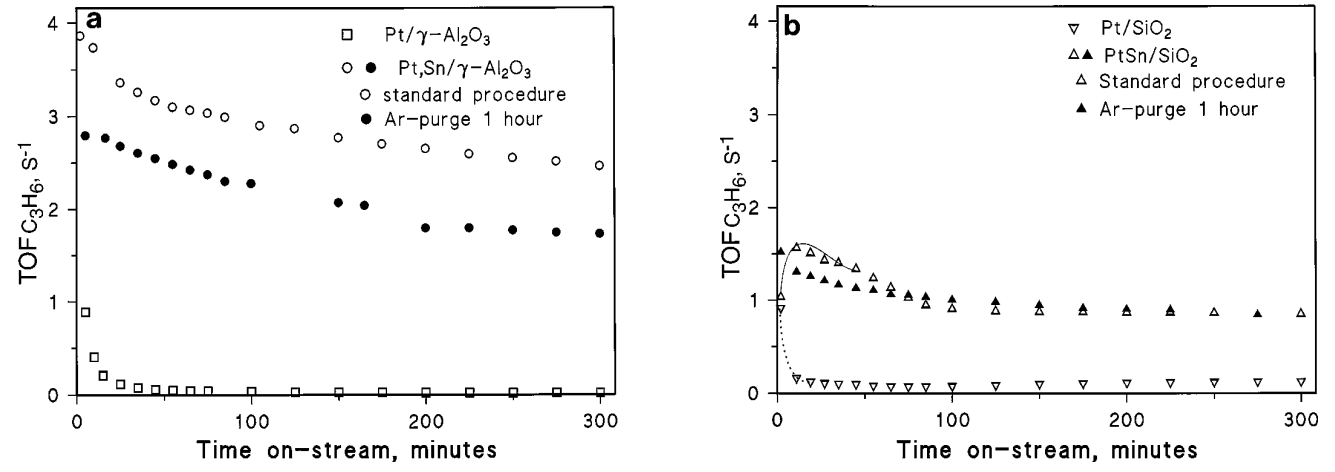

FIG. 7. Initial specific activities (TOF) of the catalysts at 519°C: (a) γ-Al_2O_3-supported catalysts, (b) SiO_2-supported samples. Conditions: WHSV = 10 h^{-1}, $C_3H_8:N_2 = 3:7$, $P_{tot} = 1$ bar.

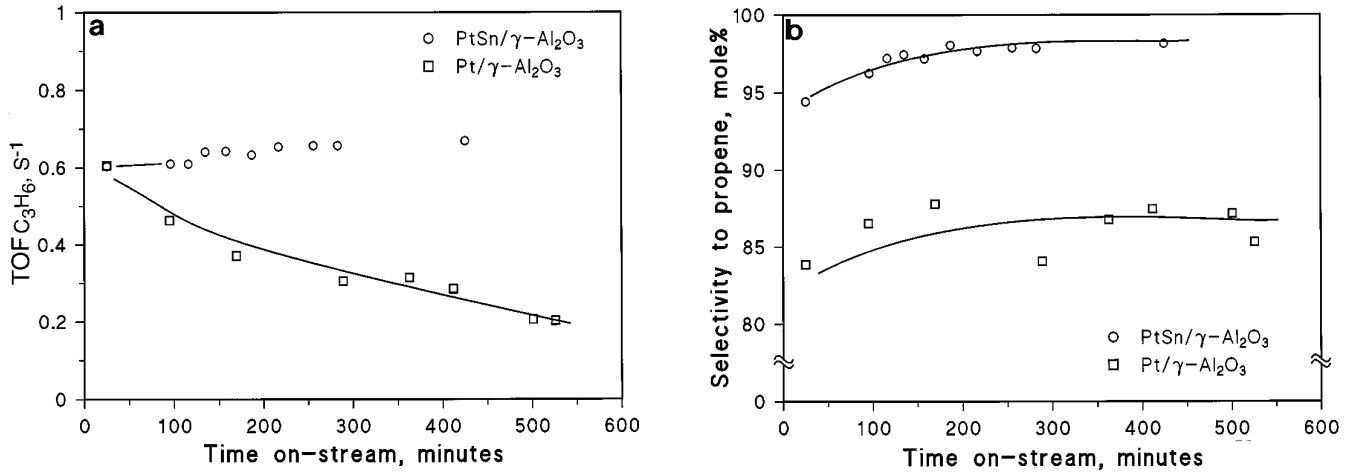

FIG. 8. (a) Initial specific activities (TOF) and (b) selectivities to C_3H_6 over the γ-Al_2O_3-supported catalysts at 519°C. Conditions: WHSV = 3.3 h^{-1}, $C_3H_8:N_2:H_2 = 3:7:1$, $P_{tot} = 1$ bar.

to the feed gas. The selectivity data shown in Fig. 8b confirm the beneficial effect of Sn on the dehydrogenation selectivity, due to reduced hydrogenolysis. Without Sn the C_3H_6 selectivity was about 85–90%, whereas with Sn this value was close to 98%. Without H_2 in the feed the cracking/hydrogenolysis pattern over the γ-Al_2O_3-supported catalysts was very sensitive to the presence of Sn. Figure 9 shows the selectivities to light products as a function of time for the two catalysts. Over the Pt/γ-Al_2O_3 acid-catalyzed cracking is important, giving C_2H_4 and H_2 in equimolar amounts, and very little C_2H_6, ascribed to metal-catalyzed hydrogenolysis. On PtSn/γ-Al_2O_3 the selectivity to light products is 1–2 orders of magnitude lower, and C_2H_6 is a major product. This could be due to direct hydrogenolysis on the metal function or due to secondary hydrogenation of C_2H_4 formed by cracking. The difference in the development of the selectivities with time shows that the side reactions on Pt/γ-Al_2O_3 (cracking) decline more slowly than the main reaction (dehydrogenation), leading to increasing selectivity for light products with time on stream. Over the PtSn/γ-Al_2O_3 this picture is reversed, leading to increasing C_3H_6 selectivity with time on-stream.

Over the SiO_2-supported samples the C_3H_6 selectivity was always very high; e.g., at 427°C no C_1–C_2 products were detected.

DISCUSSION

State of Pt and Sn in Reduced Catalysts

The brief TPR experiments included in this work (Fig. 3, Table 2) indicate that the catalysts reported here behave similarly to those studied by others. A general picture of

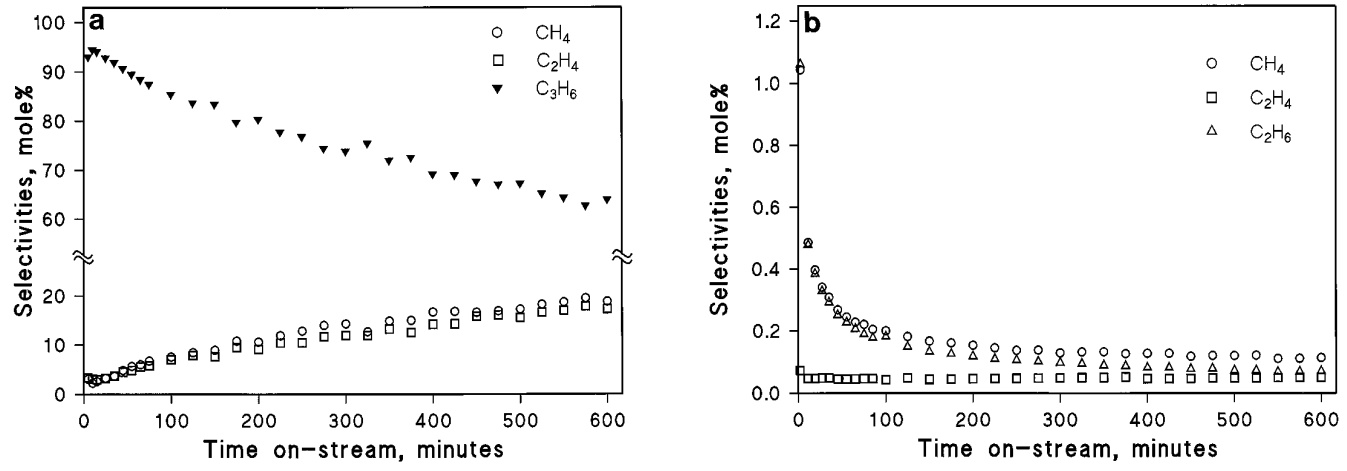

FIG. 9. Selectivities as a function of time on stream for the γ-Al_2O_3-supported catalysts: (a) Pt/γ-Al_2O_3, (b) PtSn/γ-Al_2O_3 (note the scale difference, C_3H_6 selectivity not shown, constitutes the balance to 100%). Conditions as in Fig. 7.

this class of catalysts is that Pt is easily reduced, whereas the state of Sn in PtSn catalysts is a function of support, loading, preparation method, and pretreatment conditions. When prepared by a standard impregnation technique on Al_2O_3, Sn is often found to be stabilized in an (average) oxidation state >0 (most often close to $+2$) by interaction with the support (1, 3, 5, 7, 34–38). The presence of metallic tin has not been completely ruled out, and Pt–Sn alloys have been reported on Al_2O_3, particularly if the tin loading is high or special preparation techniques have been employed. Usually only a small fraction of the Pt is found to be alloyed with metallic tin; see, e.g., Refs. (10, 11, 13). The fraction of metallic tin in $PtSn/Al_2O_3$ catalysts has been reported to increase with repeated regeneration cycles (39). On SiO_2 Sn in PtSn catalysts is readily reduced and alloys can be formed (7, 38, 39), whereas on active carbon metallic tin in a separate tin phase has been found by Mössbauer spectroscopy (39). Our TPR results fit this general pattern, and we conclude that tin is reducible and alloying is possible when PtSn is supported on SiO_2, whereas tin to a large extent is stabilized in the $+2$ state when PtSn is supported on γ-Al_2O_3. However, the precision and sensitivity of the TPR measurement does not allow the exclusion of other phenomena occurring to a small extent, and on the basis of our TPR results alone we cannot rule out the possibility that a small fraction of the tin is reduced to the metallic state also on γ-Al_2O_3. The TPR of the reoxidized samples shows that reduction–oxidation cycles influence the reduction properties. This could be very important in understanding industrial catalysts, which usually undergo multiple cycles of reduction–reaction–oxidation (coke burning) and possibly also redispersion by chloride components before reduction.

Platinum Dispersion and Chemisorption Properties

The pulse chemisorption data reported here (Table 4) show an increase in hydrogen uptake with tin addition on both supports. There is conflicting evidence in the literature regarding the effect of tin addition on the platinum dispersion. On alumina, several groups have found increased Pt dispersion (1, 7, 8, 34), but the opposite conclusion has also been reached (19, 40, 41). Metal loadings, preparation technique, and measurement technique are important parameters to consider. Gervasini and Flego (41) have shown that with the pulse technique, the measurement conditions, particularly the time between pulses and consequently the influence of the desorption kinetics, can influence the results, but not to such an extent that the wrong conclusion can be drawn with regard to comparing two related samples. Thus, we conclude that our preparation gives enhanced Pt dispersion with both Al_2O_3 and SiO_2 as supports.

The TPD profiles (Table 3) give some interesting information regarding the properties of these catalysts. After reduction and cooling in flowing H_2 very high H/Pt ratios were observed for the promoted samples. These high hydrogen uptakes could be due to spillover of hydrogen atoms to the support surface. The presence of subsurface hydrogen on Pt has also been discussed (42), but would not be expected to account for such large amounts of hydrogen. It has also been indicated that PtSn alloys can dissolve some hydrogen (29), but again, the amounts are reported to be small compared to the chemisorbed amounts. Hence, the very large desorption peaks are attributed to spillover hydrogen, as also seen by others (43, 44) for unpromoted samples. The peak temperature of 470°C for $PtSn/\gamma$-Al_2O_3 fits well with the desorption temperature of 480°C reported by Kramer and Andre (45) for atomic hydrogen on a γ-Al_2O_3 surface. The larger amount desorbed from the SiO_2-supported sample could indicate a larger capacity for spillover H on the much larger surface area of the SiO_2-supported sample, but could also be a reflection of a difference in rates of spillover in the two cases. However, in this case the desorption of hydrogen dissolved into possible PtSn phases cannot be excluded, since the desorption temperature is different.

The mechanism of the increase in spillover observed with Sn promotion is unclear. However, it has been suggested that addition of Sn leads to increased mobility of hydrogen (3). Pt sites are necessary for H_2 dissociation, and the amounts of hydrogen desorbed, corresponding to many monolayers on the available Pt, confirm that the hydrogen must be on the support surface. The density of spiltover hydrogen atoms on alumina and silica surfaces has been found to be close to 10^{12} cm^{-2} (43). Our results correspond to a density of about 3×10^{13} cm^{-2} ($PtSn/\gamma$-Al_2O_3) or 4×10^{13} cm^{-2} ($PtSn/SiO_2$), which is larger by an order of magnitude and closer to the densities measured on active carbon supports (43). This could indicate that the large amount of desorbed hydrogen should be attributed to other hydrogen species, e.g., species formed with the PtSn phase. On the other hand, as the catalytic results presented here and elsewhere show, the Sn-promoted catalysts have dramatically changed properties, and this could be linked with the ability to have reactive hydrogen available and thus reduce coking on the surface.

One important conclusion is that this experiment is unsuitable for determining Pt dispersion, as the spillover of hydrogen to the support obscures the measurement of the chemisorption on the Pt metal.

After chemisorption at 20°C the TPD profiles are quite similar for the samples (Fig. 4a). The main desorption peak is located close to 80°C and is attributed to hydrogen desorbed from metallic Pt. Pt/SiO_2 shows a very weak feature at about 265°C, and there is some desorption at the maximum temperature of the experiment, particularly for the Sn-promoted samples, possibly indicating the formation of some spiltover hydrogen even at the lower ad-

sorption temperature. After adsorption at 100°C (Fig. 5b) only the Pt/SiO_2 shows a low temperature desorption peak. The peak, located at about 165°C, corresponds to weak features observed at 150 and 200°C in the TPD after reduction and cooling in H_2 (Fig. 4). The peaks at 550°C are also smaller, indicating that they in fact stem from the initial high-temperature adsorption after reduction and cooling and not from the subsequent adsorption experiments. This shows that the combination and desorption of spiltover hydrogen is a very slow process and that spiltover hydrogen is present on the surface even after 30 min purging in Ar at 550°C.

These results show that the desorption peak about 80°C can be attributed to hydrogen adsorbed at low temperatures, probably on metallic platinum (Figs. 4 and 5). There is, however, no clear correlation between the size of this TPD peak and the amount chemisorbed using the pulse technique. All the other desorption peaks are due to adsorption or spillover processes occurring only at higher temperatures (activated processes) and the magnitude of the desorption peaks are not necessarily a measure of the metal surface of the sample. Spillover is an activated process, requiring high temperatures to occur, and it also requires certain catalytic properties, since Sn promotion leads to dramatic changes in the spillover of hydrogen.

TABLE 5

Comparison of Relative Specific Activities in Catalytic Dehydrogenation over Pt and PtSn Catalysts Supported on Al_2O_3 or SiO_2

System studied	Relative specific activity	
C_3H_8 dehydrogenation	427°C	519°C
	This work	
$0.44Pt/\gamma\text{-}Al_2O_3$	1.0	1.0
$0.35Pt–1.26Sn/\gamma\text{-}Al_2O_3$	1.2	1.0
$0.6Pt/SiO_2$	0.9	—
$0.6Pt\text{-}1.2Sn/SiO_2$	0.1	—
C_3H_8 dehydrogenation	600°C	519°C
	Yarusov *et al.* (46)	
$0.37Pt/Al_2O_3$	1.0	
$0.40Pt/SiO_2$	1.0	
$0.27Pt–0.2Sn/Al_2O_3$	0.86	
$0.56Pt–0.51Sn/Al_2O_3$	0.7	
$1.16Pt–0.71Sn/SiO_2$	0.1	
Pt–Sn (1:1) alloy	0.1	
	Dehydrogenation[a]	Aromatization[b]
	Berndt *et al.* (47)	
$0.5Pt/\eta\text{-}Al_2O_3$	1.0	1.0
$0.5Pt–0.55Sn/\eta\text{-}Al_2O_3$	0.9	5.6

[a] Cyclohexane dehydrogenation at 250°C.
[b] *n*-Heptane dehydrocyclization at 500°C.

Catalytic Activity, Selectivity and Stability

In Table 5 the initial activities from these experiments are compared to some other results from similar systems. The table shows relative data, where the specific activity of Pt/Al_2O_3 (on a TOF basis) is taken as the standard. The results from Yarusov *et al.* (46) show the same trend as our data. Furthermore, they have included PtSn alloys in their experiments, showing that a PtSn alloy surface is about one-tenth as active as the Pt alone and very similar to the $PtSn/SiO_2$ sample. Berndt *et al.* (47) report the same specific activity of Pt and PtSn on $\eta\text{-}Al_2O_3$ in cyclohexane dehydrogenation, but when the typical catalytic-reforming reaction aromatization (dehydrocyclization) of *n*-heptane to toluene was studied, they found a very different trend, with the PtSn sample being about five times more active (per surface Pt) than the unpromoted sample.

The catalytic results can be discussed in light of the understanding of the structure and state of the metals as discussed above. The well-known effects of tin as a promoter, the enhanced stability of the catalyst due to less poisoning by coke on the metal surface, and the improvement of the selectivity due to reduced cracking and hydrogenolysis are confirmed. The acid-catalyzed cracking reactions are only important on $\gamma\text{-}Al_2O_3$ and are inhibited to a large extent by Sn addition. The most significant result, however, is that the initial specific activity of Pt is the same for $Pt/\gamma\text{-}Al_2O_3$, $PtSn/\gamma\text{-}Al_2O_3$, and Pt/SiO_2, whereas $PtSn/SiO_2$ is an order of magnitude less active on a TOF basis (Fig. 6). This confirms similar results reported by others (Table 5). In other words, surface Pt atoms in $PtSn/Al_2O_3$ and surface Pt atoms in unpromoted catalysts behave similarly in this respect, whereas surface Pt in $PtSn/SiO_2$ is less active and behaves as Pt in PtSn alloys (46). This is in line with our characterization data. The TPR results show that Sn in $PtSn/SiO_2$ is close to being completely reduced, and thus alloying with Pt is possible, whereas in $PtSn/\gamma\text{-}Al_2O_3$ the Sn is only partly reduced. The difference in $PtSn/\gamma\text{-}Al_2O_3$ and $PtSn/SiO_2$ is further underlined by the purging experiments. Over the $PtSn/\gamma\text{-}Al_2O_3$ catalyst adsorbed hydrogen aids in maintaining catalyst activity (Fig. 7a), most probably by reducing coking on the metal. The initial state is important, since the activity lost initially is not regained. On the other hand, over the $PtSn/SiO_2$ the adsorbed hydrogen inhibits the reaction (Fig. 7b), indicating that the catalyst surface is different. The purged system does not deactivate faster than the system with hydrogen adsorbed. This effect has been reported by others, e.g., by Rorris *et al.* (48), studying hydrogenation, who found inhibition by strongly bound hydrogen on a Pt/SiO_2 catalyst. Rochefort *et al.* (49) recently reported a similar effect in methylcyclohexane dehydrogenation over a $Pt/\alpha\text{-}Al_2O_3$ catalyst, but they also

found a change in the deactivation profile of their catalyst. They related their data to removal of strongly bound "high-temperature hydrogen" and to restructuring of the Pt particles after longer treatments in argon. Clearly, the presence of strongly bound hydrogen is sensitive to catalyst structure and pretreatment, and its presence can influence apparent catalyst activity through blocking active sites. However, further studies are necessary to completely understand the role of this hydrogen species.

On $PtSn/SiO_2$ adsorbed hydrogen is not necessary to maintain the activity, while on $PtSn/\gamma\text{-}Al_2O_3$ purging leads to an initial loss of activity that is not recovered. This could indicate that Pt in a possible PtSn alloy on $PtSn/SiO_2$ not only has a different electronic configuration and hence a lower activity, but also that the surface Pt is located in very small clusters, possibly even as single atoms. Surface segregation of tin in PtSn alloys has been demonstrated (29, 50). Biloen *et al.* (51) showed that the active site for dehydrogenation was a single Pt atom. At the same time it is well established that coking and hydrogenolysis are structure-sensitive reactions, requiring larger ensembles (52). Hence, the results presented here confirm a model where tin is reduced to metallic tin and forms an alloy with Pt on SiO_2, whereas tin in $PtSn/\gamma\text{-}Al_2O_3$ does not form metallic tin to any significant degree. The effect of tin on $\gamma\text{-}Al_2O_3$ must be seen as a promoter of the support properties, particularly of the ability to transport chemisorbed species from the Pt surface. Sn also acts as a poison of acidic sites of the Al_2O_3 support, leading to reduced cracking. The eggshell model suggested by Adkins and Davis (35) assumes that Sn is located on the support surface in the form of a tin aluminate, with properties distinct from tin oxide, and that the altered properties of platinum are due to the influence of this surface. The enhanced hydrogen uptake for promoted catalysts as seen from TPD (Table 3) is an indication of this influence and can be described as increased hydrogen mobility (3). It is known that the enhanced stability of the PtSn system is not due to reduced coke formation but to a change in the location of the coke from the metal to the support (53). Both these factors point to the support and particularly the Pt–support interface as an important factor in determining the stability of the catalysts.

ACKNOWLEDGMENTS

Financial support for this work from the Research Council of Norway and from Statoil, both through the SPUNG programme, is gratefully acknowledged. We thank G. Carlsen and O. Tronstad for performing the surface area measurements.

REFERENCES

1. Burch, R., *J. Catal.* **71,** 348 (1981).
2. Lok, L. K., Gaidai, N. A., and Kiperman, S. L., *in* "Proceedings, 9th International Congress on Catalysis, Calgary, 1988" (M. J. Phillips and M. Ternan, Eds.), Vol. 3, p. 1261. Chem. Inst. of Canada, Ottawa, 1988.
3. Sachdev, A., and Schwank, J., *in* "Proceedings, 9th International Congress on Catalysis, Calgary, 1988" (M. J. Phillips and M. Ternan, Eds.), Vol. 3, p. 1275. Chem. Inst. of Canada, Ottawa, 1988.
4. Margitfalvi, J. L., Hegedüs, M., and Tálas, E., *J. Mol. Catal.* **51,** 279 (1989).
5. Sexton, B. A., Hughes, A. E., and Foger, K., *J. Catal.* **88,** 466 (1984).
6. Li, Y.-X., Klabunde, K. J., and Davis, B. H., *J. Catal.* **128,** 1 (1991).
7. Meitzner, G., Via, G. H., Lytle, F. W., Fung, S. C., and Sinfelt, J. H., *J. Phys. Chem.* **92,** 2925 (1988).
8. Balakrishnan, K., and Schwank, J., *J. Catal.* **127,** 287 (1991).
9. Stencel, J. M., Goodman, J., and Davis, B. H., *in* "Proceedings, 9th International Congress on Catalysis, Calgary, 1988" (M. J. Phillips and M. Ternan, Eds.), Vol. 3, p. 1291. Chem. Inst. of Canada, Ottawa, 1988.
10. Srinivasan, R., Rice, L. A., and Davis, B. H., *J. Catal.* **129,** 257 (1991).
11. Srinivasan, R., De Angelis, R. J., and Davis, B. H., *Catal. Lett.* **4,** 303 (1990).
12. Bacaud, R., Bussière, P., and Figueras, F., *J. Catal.* **69,** 399 (1981).
13. Li, Y.-X., and Klabunde, K. J., *J. Catal.* **126,** 173 (1990).
14. Fan, Y., Xu, Z., Zang, J., and Lin, L., *Stud. Surf. Sci. Catal.* **68,** 683 (1991).
15. Blekkan, E. A., Holmen, A., and Vada, S., *Acta. Chem. Scand.* **47,** 275 (1993).
16. Lieske, H., Lietz, G., Spindler, H., and Völter, J., *J. Catal.* **81,** 8 (1983).
17. Kummer, J. T., *J. Phys. Chem.* **90,** 4747 (1986).
18. Dautzenberg, F. M., Helle, J. N., Biloen, P., and Sachtler, W. M. H., *J. Catal.* **63,** 119 (1980).
19. Lieske, H., and Völter, J., *J. Catal.* **90,** 96 (1984).
20. Del Angel, G., Tzompantzi, F., Gomez, R., Baronetti, G., de Miguel, S., Scelza, O. A., and Castro, A., *React. Kinet. Catal. Lett.* **42,** 67 (1990).
21. De Miguel, S. R., Baronetti, G. T., Castro, A. A., and Scelza, O. A., *Appl. Catal.* **45,** 61 (1988).
22. Burch, R., and Garla, L. C., *J. Catal.* **71,** 360 (1981).
23. Muller, A. C., Engelhard, P. A., and Weisang, J. E., *J. Catal.* **56,** 65 (1979).
24. Burch, R., and Mitchell, A. J., *Appl. Catal.* **6,** 121 (1983).
25. Ebitani, K., and Hattori, H., *Bull. Chem. Soc. Jpn.* **64,** 2422 (1991).
26. Lietz, G., Lieske, H., Spindler, H., Hanke, W., and Völter, J., *J. Catal.* **81,** 17 (1983).
27. Anderson, J. R., "Structure of Metallic Catalysts." Academic Press, London, 1975.
28. Völter, J., Lietz, G., Uhlemann, M., and Hermann, M., *J. Catal.* **68,** 42 (1981).
29. Verbeek, H., and Sachtler, W. M. H., *J. Catal.* **42,** 257 (1976).
30. Wilson, G. R., and Hall, W. K., *J. Catal.* **17,** 190 (1970).
31. Freel, J., *J. Catal.* **25,** 149 (1972).
32. Wilson, G. R., and Hall, W. K., *J. Catal.* **24,** 306 (1972).
33. Bariås, O. A., Holmen, A., and Blekkan, E. A., in preparation.
34. Schwank, J., Balakrishnan, K., and Sachdev, A., *Stud. Surf. Sci. Catal.* **75,** 905 (1993).
35. Adkins, S. R., and Davis, B. H., *J. Catal.* **89,** 371 (1984).
36. Zhou, Y., and Davis, S. M., *Catal. Lett.* **15,** 51 (1992).
37. Li, Y. X., Stencel, J. M., and Davis, B. H., *Appl. Catal.* **64,** 71 (1990).
38. Chiu, N.-S., Lee, W.-H., Li, Y.-X., Bauer, S. H., and Davis, B. H., *Stud. Surf. Sci. Catal.* **50,** 147 (1989).
39. Yang, W., Lin, L., Fan, Y., and Zang, J., *Catal. Lett.* **12,** 267 (1992).
40. Lin, L., Zhang, T., Zang, J., and Xu, Z., *Appl. Catal.* **67,** 11 (1990).
41. Gervasini, A., and Flego, C., *Appl. Catal.* **72,** 153 (1991).
42. Christmann, K. R., *in* "Hydrogen Effects in Catalysis" (Z. Paál and P. G. Menon, Eds.), Chemical Industries Vol. 31, p. 3. Dekker, New York, 1988.

43. Conner, W. C., Jr., *in* "Hydrogen Effects in Catalysis" (Z. Paál and P. G. Menon, Eds.), Chemical Industries Vol. 31, p. 311. Dekker, New York, 1988.
44. Altham, J. A., and Webb, G., *J. Catal.* **18,** 133 (1970).
45. Kramer, R., and Andre, M., *J. Catal.* **58,** 287 (1979).
46. Yarusov, I. B., Zatolokina, E. V., Shitova, N. V., Belyi, A. S., and Ostrovskii, N. M., *Catal. Today* **13,** 655 (1992).
47. Berndt, V. H., Mehner, H., Völter, J., and Meisel, W., *Z. Anorg. Allg. Chem.* **429,** 47 (1977).
48. Rorris, E., Butt, J. B., Burwell, R. L., Jr, and Cohen, J. B., *in* "Proceedings, 8th International Congress on Catalysis, Berlin, 1984," Vol. 4, p. 321. Dechema, Frankfurt-am-Main, 1984.
49. Rochefort, A., Le Peltier, F., and Boitiaux, J. P., *J. Catal.* **145,** 409 (1994).
50. van Santen, R. A., and Sachtler, W. M. H., *J. Catal.* **33,** 202 (1974).
51. Biloen, P., Helle, J. N., and Sachtler, W. M. H., *J. Catal.* **58,** 95 (1979).
52. Ribeiro, F. H., Bonivardi, A. L., Kim, C., and Somorjai, G. A., *J. Catal.* **150,** 186 (1994).
53. Liu, J., Gao, X., Zhang, T., and Lin, L., *Thermochim. Acta* **179,** 9 (1991).